Evaluation of Resin Molds Change in Design and Polymerization by Using a Wavefront Sensor

Kazumasa Tatsumi[1,2][a], Kentaro Saeki[1][b], Shin Kubota[1], Yoshikatsu Kaneda[1], Kenji Uno[1,3],
Kazuhiko Ohnuma[1,3] and Tatsuo Shiina[2][c]

[1]SEED CO., LTD, 2-40-2 Hongo, Bunkyo-ku, Tokyo, 369-0131, Japan
[2]Chiba University, 1-33 Yayoi-cho, Inage-ku, Chiba-shi, Chiba, 263-8522, Japan
[3]Laboratorio de Lente Verde, 98-1 Nozomino, Sodegaura, Chiba, 299-0251, Japan

Keywords: Wavefront Sensor, Wavefront Shape, Contact Lenses, Resin, Mold.

Abstract: Advances in molding technology have made it possible to produce plastic molded products with complex shapes. In contact lens manufacturing, a double-sided molding method using resin molds is employed, where the front and back designs are replicated through injection molding. However, shape changes in the resin molds caused by heat treatment (polymerization) during the manufacturing process affect lens characteristics. This study proposes a method using optical techniques to clarify the influence of mold design and polymerization on resin mold shapes. Five types of resin molds were measured using a wavefront sensor, which allows for high-accuracy, non-contact measurement. Wavefront aberrations and radii of curvature were evaluated, and results showed that polymerization caused slight deviations from the design values and changes in shrinkage rates. This method demonstrated its effectiveness in measuring and evaluating resin molds for contact lens production. Furthermore, the proposed method has wide-ranging applications, including quality control in lens manufacturing and evaluating the transfer accuracy of metal molds.

1 INTRODUCTION

Injection molding technology, which has been rapidly advancing in recent years, is one of the most important technologies in the plastics industry. Since John W. Hyatt invented the vertical celluloid molding machine in 1872, laying the foundation for injection molding, the technology has seen significant growth, especially in the latter half of the 20th century (Rosato, 2000). Innovations in both injection molding techniques and plastic materials have greatly enhanced production efficiency (Ciofu, 2013). The introduction of automatic control systems using microprocessors has made it possible to manufacture parts with even greater complexity and precision. Since the 1990s, injection molding has become more refined and has evolved into a technology widely used in fields such as medical devices and electronic components.

Contact lenses are one of the medical devices manufactured using injection molding technology. In a world where myopia is increasing due to the widespread use of smartphones and other tiny small display devices, the global demand for contact lenses is rising year by year. Consequently, there is a need to mass-produce and high-quality contact lenses. The concept of contact lenses was first introduced by Leonardo da Vinci in 1508, and later in 1888, Adolf Fick developed a glass scleral lens, marking the first step toward their practical use (Oswald, 2008). Similar to the advancements in injection molding, the development of plastic materials also had a significant impact on contact lenses, leading to the creation of plastic scleral lenses, which greatly reduced their weight and improved their durability (Ciofu, 2013). In the 1960s, soft contact lenses made from hydrogel materials, developed by Otto Wichterle and Drahoslav Lim, were introduced and remain popular today (Oswald, 2008).

[a] https://orcid.org/0009-0008-2975-7695
[b] https://orcid.org/0000-0002-4902-3110
[c] https://orcid.org/0000-0001-9292-4523

Injection molding technology and contact lens manufacturing are closely related. While glass lenses are hand-polished, plastic soft contact lenses are produced using a cast molding method that utilizes a mold created through injection molding (Chen, 2017). A metal mold is made to replicate the front and back designs, and a resin mold is then produced through injection molding. The contact lenses are formed by pouring the lens material into two resin molds and fitting them together.

In the cast molding method, the surface of the resin mold must be precisely and smoothly formed to improve the quality of contact lenses (Chen, 2017). Since the raw material for contact lenses is liquid, a solid lens is formed through a heat treatment (polymerization). Polymerization is carried out by pouring the raw material into the resin mold and sealing it. The space within the fitted resin mold determines the shape of the contact lens, making the precision of the mold surface crucial. Therefore, both the mold design and the molding conditions during manufacturing are key factors in producing high-quality contact lenses, and research has been conducted to optimize these conditions (Chen, 2017) (Chang, 2001).

In mass production, resin molds are created under nearly identical basic molding conditions, but differences in precise design should still be evaluated. Additionally, the influence of the polymerization on the resin mold during the manufacturing process must also be considered. This is because plastic, the primary material for resin molds today, is more prone to deform than glass or metal, and can change shape when exposed to high temperature, around 100°C. Resin molds are typically evaluated by using a compact laser interferometer, but since the measurements rely on the person interpreting the interference fringes displayed during the measurement, quantitative assessments are not possible, and differences among them can arise.

In this study, we propose a method for evaluating resin molds using a wavefront sensor to quantitatively perform high-precision inspections. The wavefront sensor allows for highly accurate wavefront measurements at the sub-nanometer level using Zernike polynomials. Additionally, it can acquire aberration data within a few milliseconds, allowing the detection of aberration changes real-time (Atchison, 2005). Zernike coefficients can be displayed as numerical parameters, providing detailed measurements of the resin mold's aberrations. Additionally, the radius of curvature can be measured simultaneously, making the wavefront sensor a promising alternative to interferometers.

Previous research has demonstrated that measurements obtained from wavefront sensors function effectively as evaluation indices for aspheric lenses (Cheng, 2020). Given the high precision of the measurement parameters, this study utilizes the wavefront sensor to measure both the aberrations and the radius of curvature of the resin molds. This study aims to clarify how the design and polymerization during the manufacturing process affect changes in the aberration and radius of curvature of the resin molds. It enables measurements with the same accuracy as conventional measurement of interferometer, while also providing real-time, stable measurements. Therefore, it is innovative not only for contact lens manufacturing but also for quality control in medical devices and precision molded products.

2 EXPERIMENTS

2.1 Experimental Equipment

Table 1 shows an overview of the wavefront sensor used in this study. This device was specifically designed to measure the reflected wavefront of resin molds (Pulstec Industrial Co., Ltd.: LUCAS). Figure 1 illustrates the measurement principle. It employs the Shack-Hartmann principle, using either a Charge Coupled Device (CCD) or a Complementary Metal Oxide Semiconductor (CMOS) as the imaging element, which is composed of many microlenses (Atchison, 2005). A laser is irradiated from the light source, and the reflected light from the measurement object passes through the microlenses and is directed to the imaging element. As shown in Figure 2, if there is no distortion in the wavefront of the measurement object, equally spaced focused spots are formed on the imaging surface according to the arrangement of the microlenses. On the other hand, if the wavefront is disturbed due to a phase change caused by the measurement object, the incident direction of the light beam changes due to the arrangement of each lens, resulting in irregular Hartmann spot positions. Information about the shape of the incident wavefront can be obtained from this change in position. Its information of the Hartmann spots is then expressed using Zernike polynomials, which are orthogonal polynomials defined on a unit circle. Each Zernike polynomial represents an independent wavefront shape, corresponding to a specific type of aberration (Matsuyama, 2004).

Using Zernike polynomials $Z_n^m(X,Y)$, the incident equiphase surface is expressed as shown in Equation (1).

$$W(X,Y) = \sum_{i=0}^{n} \sum_{j=0}^{i} c_i^{2j-1} Z_i^{2j-1}(X,Y) \qquad (1)$$

c_i^{2j-1} represents the coefficients corresponding to each term of the Zernike polynomials. These coefficients indicate the contribution of each term to the wavefront aberration. The larger the value of c_i^{2j-1} is, the greater the influence of the corresponding Zernike term on the shape of the wavefront is.

If the displacement of the Hartmann spot is represented by $(\Delta x, \Delta y)$ and the focal length of the microlens array is f, the relationship of the wavefront position shift is expressed in Equation (2).

$$\frac{\partial W(X,Y)}{\partial X} = \frac{\Delta x}{f} \quad \frac{\partial W(X,Y)}{\partial Y} = \frac{\Delta y}{f} \qquad (2)$$

The wavefront can be reconstructed by substituting Equation (1) into Equation (2) to obtain the Zernike coefficients.

Table 1: Specification of the wavefront sensor.

| Index	Parameter
Manufacturer	Pulstec Industrial Co., Ltd.
Model	LUCUS
Measurement wavelength	589 nm
Measurement range of concave surface	4.3 mm~46.5 mm
Measurement range of convex surface	5.7 mm~9.5 mm
Tolerance of wavefront incident angle	±1.1 deg
Wavefront measurement accuracy	1/100 λ
Repeatability	1/200 λ
Radius measurement accuracy	±10 μm
Number of microlens array	108×80
The focal length of the microlens array	4 mm
Data update rate	6 Hz
Focal lens	NA 0.81
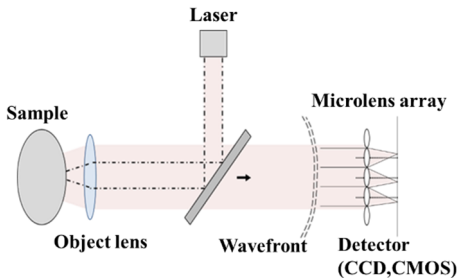
Figure 1: Wavefront sensor principle.
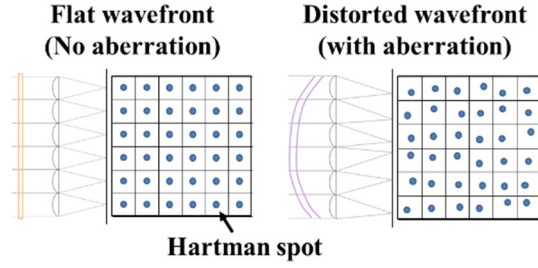
Figure 2: Relationship between wavefront and Hartmann spot.

2.2 Zernike Polynomials

In this study, the resin mold was evaluated using Zernike coefficients. The device can output 36 Zernike coefficients, but this study focused on the unique ones. Zernike coefficients are widely used in ophthalmic optics and are often employed to assess ocular aberrations (Salmon, 2006). The Zernike polynomials were standardized by fringe order (Niu, 2022). Among the Zernike coefficients shown in Table 2, "Z04" and "Z07" exhibited the largest changes.

"Z04" indicates astigmatism, which is one of the five types of Seidel aberrations (spherical aberration, coma aberration, astigmatism, field curvature, and distortion aberration) (Carvalho, 2005). When the orthogonal coordinates in an optical system are defined as the horizontal and vertical planes, astigmatism occurs when there is a shift between the focal positions of the light beam in these planes. The resulting image can be an ellipse, a circle, or a line. In optical lenses, astigmatism arises when the horizontal and vertical radii of curvature differ.

"Z07" indicates coma aberration, which occurs when light incident at an angle does not converge to a single point on the image plane, resulting in a conical image. This aberration is influenced by the distance from the optical axis, significantly affecting how the image appears through the lens.

Table 2: Zernike polynomials.

Term	Polynomial	Aberration
Z01	$\rho\cos\theta$	x-Tilt
Z02	$\rho\sin\theta$	y-Tilt
Z03	$2\rho^2 - 1$	Defocus
Z04	$\rho^2 \cos2\theta$	0°Primary astigmatism
Z05	$\rho^2 \sin2\theta$	45°Primary astigmatism
Z06	$(3\rho^2 - 2)\rho \cos\theta$	Primary x-coma
Z07	$(3\rho^2 - 2)\rho \sin\theta$	Primary y-coma
Z08	$6\rho^4 - 6\rho^2 + 1$	Primary spherical aberration
Z09	$\rho^3 \cos3\theta$	Secondary x-trefoil
Z10	$\rho^3 \sin3\theta$	Secondary y-trefoil

Both of these aberrations are critical components in the creation of contact lenses, and the manufacturing process must be designed to minimize their presence. By understanding that these aberrations exist in resin molds, their relationship to contact lens aberrations can be clarified.

2.3 Measurement Sample

2.3.1 Contact Lens

Figure 3 shows an overview of the contact lens. In this study, the contact lens and the resin mold were measured. The refractive power of the lens is adjusted by designing the radius of curvature. This range is called the Optical Zone (OZ) and plays an important role in vision correction with contact lenses. The lens made in this study was designed with an OZ of φ5.77 mm, and the radius of curvature was variable (OZ radius). The five different curvature radii were prepared in Table 3. The design outside the OZ was common to all patterns, with the radius of curvature changed in two stages. The back surface was designed with a single radius of curvature, R = 6.670[mm], which was also common to all patterns.

The contact lenses were measured using the NIMO TR1504 manufactured by Lambda-X Ophthalmic. This device employs a technology that combines interferometry and phase-shifting technology using the Phase-Shifting Schlieren (PSS) method (Joannes, 2003). It can measure the power profile and wavefront aberration of contact lenses. Although this device can't measure wavefront measurement of resin molds, it's useful for evaluating contact lenses.

2.3.2 Resin Mold

Figure 4 shows an overview of the fitted state of the resin molds. The design of the concave side for the lens front (the orange part in the figure) was valuable as shown in Table 3. And the measurement results with the interferometer are presented as well. The OZ radius was adjusted in 0.500 mm increments. The measurement range was diameter of 5 mm from the center of the concave surface. All resin molds for the back surface maintained the same design. The measurement range of the convex surface was the same as the concave one. The reflectivity of the mold may potentially affect the measurements taken by the wavefront sensor. Adjusting the laser power on the measurement device, it is possible to eliminate the influence of reflectivity. In this study, the saturated pixels of the Hartmann spot were defined, and the

laser power was adjusted to ensure that the number of pixels was within the specified range.

2.3.3 Polymerization

Contact lens raw materials are liquid, so solid contact lenses are formed through polymerization. Polymerization is carried out after pouring the raw materials into a resin mold and fitting it into the mold. The shape of a contact lens is defined by the gap between two resin molds. However, if the molds deform during polymerization, it can greatly impact the final lens shape.

The polymerization is crucial in forming contact lenses, and since it's closely related to their quality, polymerization was conducted in nitrogen at 105±5℃ for 120 minutes, which simulates the conditions during actual polymerization.
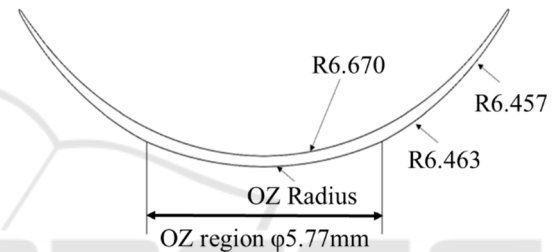

Figure 3: Overview of the contact lens.

Table 3: Specification of resin molds.

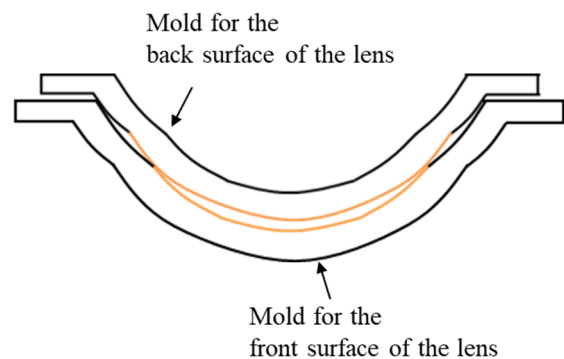| Sample No.	Value of OZ radius[mm]	Measurement of Interferometer [mm]
A	6.500	6.476
B	7.000	6.975
C	7.500	7.441
D	8.000	7.899
E	8.500	8.378

Figure 4: Overview of the resin mold.

3 RESULT

3.1 Zernike Coefficients

Wavefront measurements were performed on five samples with different OZ radius design values. Five measurements were taken for each sample. As a result, for Z07, the design-dependent changes in the Zernike coefficients were confirmed before and after polymerization. The comparison results before and after polymerization are presented shown in Figure 5(a) ~ (c).

Figure 5(a) shows the measurement results before polymerization. The horizontal axis represents the Zernike coefficient terms, and the vertical axis displays the Zernike coefficient values. This device can output 36 Zernike coefficients. However, since there is almost no change from Z10 onwards, they were judged to be unnecessary for evaluating the resin mold. It was found that Z04 exhibited different values depending on the OZ radius design. Similarly, the difference in Z07 represented different designs. Although the difference in the measurement results due to the design for Z06 was small, it was still possible to observe the variation in the results, while Z10 didn't change regardless of the design.

Figure 5(b) shows the measurement results for the resin mold after polymerization. The sample shown in Figure 5(a) was heat-treated under the conditions specified in Section 2.3.3, and after the polymerization, it was measured again using a wavefront sensor. The absolute values of each coefficient became larger than before the polymerization. Z07 changed regularly. Z04 and Z05 changed significantly, but the results showed a large variance.

Figure 5(c) shows the changes in each coefficient before and after polymerization. The changes were calculated by subtracting the Zernike coefficient values before polymerization from after polymerization. It was found that the coefficient values were generally larger after polymerization. Z04's values shifted in the negative direction, although there was some variance. Z07's values increased overall, showing a tendency for the amount of change in value to depend on the OZ radius design. For the other values, Z05 exhibited a larger variance, while the other coefficients showed that the Zernike coefficients increased in absolute values.
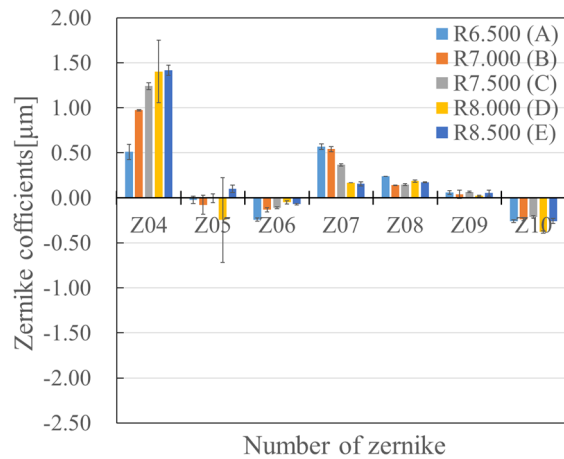

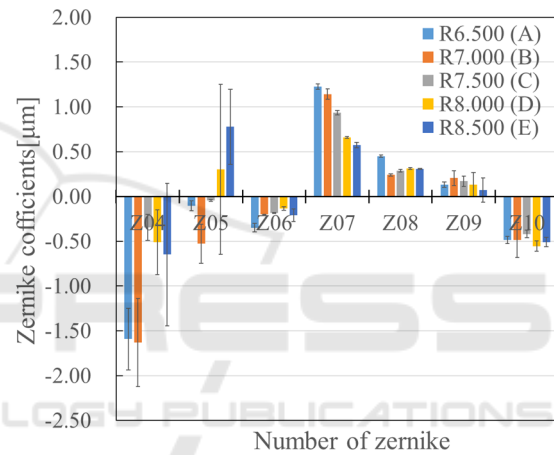Figure 5(a): Zernike coefficients before polymerization.

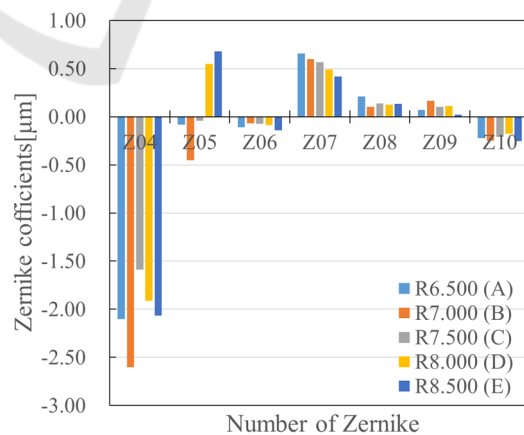Figure 5(b): Zernike coefficients after polymerization.

Figure 5(c): Change in subtraction for Zernike coefficients.

3.2 Oz Radius

Figure 6 shows the measurement results of the radius of curvature compared to the design value of the OZ radius of the resin mold. The horizontal axis represents the design value, while the vertical axis represents the measured value. This comparison illustrates the differences before and after polymerization for each design.

Table 4 presents the measurement results and deviations from the design value. The radius of curvature was consistently smaller than the design value, with the deviation increasing as the design value of OZ radius increased.

Table 5 shows the measurement results and shrinkage rates of the radius of curvature before and after polymerization. The radius of curvature before polymerization was equivalent to the values with the interferometer shown in Table 3. And it was found that the radius of curvature shrank further after polymerization compared to before polymerization. The measurement results also indicated that the larger the design value of the OZ radius is, the greater the shrinkage rate is, too. The polymerization-induced shrinkage further increased the difference between the radius of curvature of the resin mold and the design value.

Table 4: Difference in design value.

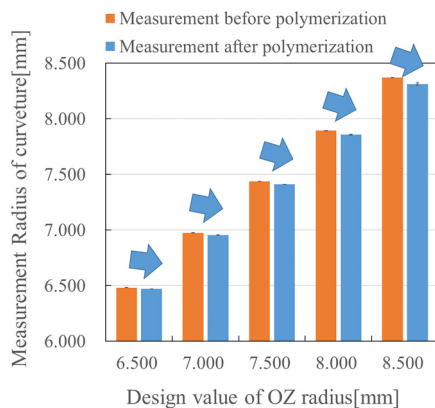| Value of OZ radius [mm]	Measurement OZ radius before polymerization [mm]	Difference from design value [%]
6.500 (A)	6.482	0.3%
7.000 (B)	6.976	0.3%
7.500 (C)	7.439	0.8%
8.000 (D)	7.895	1.3%
8.500 (E)	8.371	1.5%

Figure 6: Change in each measurement radius.

Table 5: Shrinkage rate due to polymerization.

Value of OZ radius [mm]	Measurement OZ radius before polymerization [mm]	Measurement OZ radius after polymerization [mm]	Shrinkage Rate [%]
6.500 (A)	6.482	6.471	0.17%
7.000 (B)	6.976	6.956	0.29%
7.500 (C)	7.439	7.411	0.38%
8.000 (D)	7.895	7.858	0.47%
8.500 (E)	8.371	8.313	0.69%

4 DISCUSSION

In this study, we proposed the method using the wavefront sensor to evaluate resin molds used in contact lens manufacturing. Specifically, we measured the Zernike coefficients and radius of curvature for five types of resin molds with different curvature radii in the OZ range, to assess the impact of each design difference on aberrations. We also compared the measurement results before and after the polymerization performed during the manufacturing process to observe changes in aberrations and the radius of curvature.

The difference in the curvature radius of the OZ range caused a significant change in Z07 (coma aberration), clearly indicating that design variations affect aberrations. In contrast, changes in Z04 (astigmatism) will be largely influenced by polymerization conditions, likely due to the characteristics of the material.

Furthermore, after comparing the changes in Zernike coefficients, we found the overall increase in aberration values with the most significant change observed in Z07. This means that the interaction between design and polymerization has an influence on the aberrations of the resin mold. As similar study, Cheng et al. (Cheng, 2020) also used a wavefront sensor to evaluate aberrations and analysed the impact of molding errors on the optical performance of lenses. Both studies share the common approach of evaluating molding errors based on Zernike coefficients and are considered effective methods for quantitatively assessing molding errors during the manufacturing process.

In addition, contact lenses were produced using the resin molds made in this study, and their measurements were performed using the NIMO TR1504. The evaluation range was φ5.0 mm. Table 6 shows the measured radius of curvature of the resin molds. Each lens refractive power was calculated using that radius of curvature. Furthermore, each power of contact lenses was measured by NIMO. The

data on Table 6 are also plotted in Figure 7. The horizontal axis represents the design value of the radius of curvature, and the vertical axis is the refractive power. Both the theoretical lens power and the measured lens power were shown on the graph.

The results of this study indicate that sample C had almost no error in lens power, confirming that the lens was produced as designed. In contrast, samples A and E showed differences from the design values. The difference in the radius of curvature between the front and back surfaces of the resin mold (maximum and minimum values) likely caused an imbalance in the resin thickness between the center and periphery, which affected the shrinkage. On the other hand, the resin thickness of sample C showed a thickness difference of less than 10μm between the center and periphery, which was more uniform compared to the other samples. As a result, sample C was the most accurately produced according to the design. Based on these findings, to further investigate the effects of polymerization, it is necessary to accurately measure the thickness of the resin mold. As a method for measuring transparent resin mold, there are some reports about the measurement method of contact lenses with Optical Coherence Tomography (OCT) principles (Saeki, 2020, 2021). OCT measurements can provide data on the thickness of the resin mold and the front and back curvature radii inside and outside the OZ range. While the wavefront sensor can measure wavefront shape and curvature radius with high precision, it cannot measure the thickness or the shape of the back surface of the resin mold. The impact of resin thickness is a factor in the inability to manufacture the lenses as designed. Therefore, by adding data on changes in resin thickness obtained through OCT measurements, we can clarify the influence of resin thickness on the lenses. By combining the results of this study with OCT data, it becomes possible to assess the impact of the non-uniformity of resin thickness on shrinkage and lens power. These results can provide appropriate feedback into the design as manufacturing factors.

Table 6: Comparison of theoretical and measured values of OZ radius and refractive power.

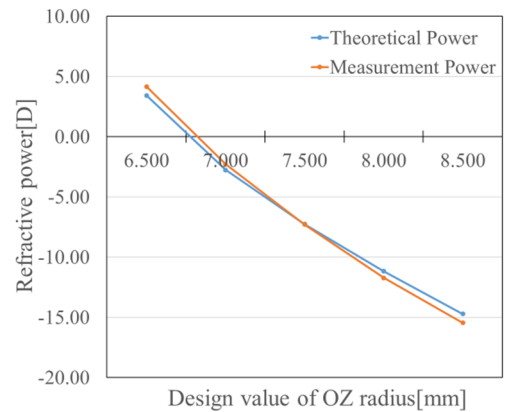| Value of OZ radius [mm]	Measurement OZ radius after polymerization [mm]	Theoretical value of refractive power [D]	Measurement refractive power [D]
6.500 (A)	6.471	+2.73	+4.16
7.000 (B)	6.956	-2.76	-2.28
7.500 (C)	7.411	-7.26	-7.29
8.000 (D)	7.858	-11.16	-11.72
8.500 (E)	8.313	-14.72	-15.44

Figure 7: Variation of theoretical and measured values of OZ radius and refractive power.

In this study, the evaluation was limited to five types of resin molds, but more diverse designs and different molding conditions are necessary for a comprehensive understanding. Additionally, experiments under varying temperatures and durations could provide more detailed insights into the influence of polymerization. Although the wavefront sensor used in this study enables highly precise measurements, comparative verification with other measurement methods remains a future challenge.

It is anticipated that the evaluation method using the wavefront sensor will be applied to other materials and molding processes, further expanding its general applicability. In particular, this method can be applied to the evaluation of transfer accuracy in precise resin molding such as medical devices. Cheng et al.'s research (Cheng, 2020) evaluated aberrations in the manufacturing process of mobile phone camera lenses and contributed to the optimization of manufacturing conditions. By optimizing the manufacturing process based on the Zernike coefficients obtained in this study, the mass production of higher-quality contact lenses will become feasible. In this way, the wavefront sensor-based evaluation method can be applied to quality control across various optical products, including contact lenses.

5 SUMMARY

In this study, the wavefront sensor was used to evaluate resin molds utilized in contact lens manufacturing. Five types of resin molds that have each different curvature radius in the OZ range were measured. Wavefront measurements were also

conducted before and after polymerization to observe their changes.

The clear trend was observed in the measurement results due to differences of the radii of curvature in the OZ range, and specific Zernike coefficients were identified. It was also confirmed that the certain Zernike coefficients Z04 and Z07 changed after polymerization.

Additionally, the measurement results for the radius of curvature showed values smaller than the design values even before polymerization. Polymerization caused the resin molds to shrink more, making the radius of curvature even smaller. It was found that the larger the design value is, the greater the shrinkage rate is, too, which is leading to a larger difference from the design value.

The results for the radius of curvature were shown to be consistent with those obtained using a laser interferometer, demonstrating that changes in aberration due to differences in the resin mold design could be effectively evaluated using Zernike coefficients of Z01 - Z10 as parameters. This suggests that the wavefront sensor is a useful new method for evaluating those resin molds.

However, for the contact lenses produced using the resin molds from this study, there was a difference between the lens power derived from the measured radius of curvature of the resin molds and the actual lens power measured by NIMO. The exact cause related to the transfer accuracy from the resin mold to the contact lens remains unclear and will be a subject of future investigation. There have already been reports on methods for evaluating the shape of contact lenses using OCT (Saeki, 2021). By combining the results from these methods, further evaluation of the lenses will be investigated the correlation between the transfer accuracy of the resin mold and the final contact lens.

REFERENCES

Rosato, D. V., Rosato, D. V., & Rosato, M. G. (2000). *Injection molding handbook*. Kluwer Academic Publishers.

Ciofu, C., & Mindru, D. T. (2013). Injection and micro injection of polymeric plastics materials: A review. *International Journal of Modern Manufacturing Technologies*, 5(2), 21-30.

Oswald, T. A., Turng, L.-S., & Gramann, P. J. (2008). *Injection molding handbook* (2nd ed.). Hanser Verlag.

Chen, C.-C. A., et al. (2017). Study on injection molding of shell mold for aspheric contact lens fabrication. *Procedia Engineering*, 184, 344–349.

Chang, T. C., & Faison, E. (2001). Shrinkage behavior and optimization of injection molded parts studied by the Taguchi method. *Polymer Engineering and Science*, 41(5), 703-709.

Atchison, D. A. (2005). Recent advances in measurement of monochromatic aberrations of human eyes. Clinical and Experimental Optometry, 88(1), 5-27.

Cheng, X., Yan, L., Liu, L., Cao, J., Lin, Y. J., & Hao, Q. (2020). Fabrication-error analysis of injection-molded aspheric elements using typical aberration terms in transmitted wavefront with Shack–Hartmann wavefront-sensing measurement. *Optical Engineering*, 59(12), 123102.

Matsuyama, T., & Ujike, T. (2004). Orthogonal aberration functions for microlithographic optics. Optical review, 11(4), 199-207.

Salmon, T. O., & van de Pol, C. (2006). Normal-eye Zernike coefficients and root-mean-square wavefront errors. Journal of Cataract & Refractive Surgery, 32(12), 2064-2074.

Niu, K., & Tian, C. (2022). Zernike polynomials and their applications. *Journal of Optics*, 24(12), 123001.

Carvalho, L. A. (2005). Accuracy of Zernike polynomials in characterizing optical aberrations and the corneal surface of the eye. Investigative ophthalmology & visual science, 46(6), 1915-1926.

Joannes, L., Dubois, F., & Legros, J.-C. (2003). Phase-shifting schlieren: High-resolution quantitative schlieren that uses the phase-shifting technique principle. *Applied Optics*, 42(25), 5046–5053.

Saeki, K., Huyan, D., Sawada, M., Sun, Y., Nakamura, A., Kimura, M., ... & Shiina, T. (2020). Measurement algorithm for real front and back curved surfaces of contact lenses. Applied Optics, 59(28), 9051-9059.

Saeki, K., Huyan, D., Sawada, M., Nakamura, A., Kubota, S., Uno, K., ... & Shiina, T. (2021). Three-dimensional measurement for spherical and nonspherical shapes of contact lenses. Applied optics, 60(13), 3689-3698.

Saeki, K., Huyan, D., Nakamura, A., Kubota, S., Uno, K., Ohnuma, K., & Shiina, T. (2021). 2D and 3D Measurement Algorithms for Real Front and Back Curved Surfaces of Contact Lenses. In PHOTOPTICS (pp. 73-80).